JOURNAL OF OPTOELECTRONICS AND ADVANCED MATERIALS, Vol. 11, No. 12, December 2009, p. 2159 - 2166

Structural and optical analysis of superimposed bismuth and antimony oxides

S. CONDURACHE-BOTA*, G. I. RUSU[a], N. TIGAU, V. NICA[a], R. DRASOVEAN
Dunarea de Jos University of Galati, Romania
[a]Al. I. Cuza University of Iasi, Romania

Bismuth trioxide and antimony trioxide were deposited by thermal vacuum evaporation one on top of the other. The temperature of the substrate during deposition was maintained at 20^0 C, 70^0 C and 120^0 C, respectively. Also, the deposition order of the two oxides was reversed, in order to find if there is any change in the properties of the entire two oxides structure. Their structural characteristics were studied by means of X-ray diffraction and compared to literature. The optical transmission spectra were also studied by means of the Swanepoel and Wemple-DiDomenico methods. Clear correlations between the optical behavior and the structural changes were noticed.

(Received July 5, 2009; accepted November 12, 2009)

Keywords: Oxides, Vacuum thermal deposition, Diffractometry, Optical spectra

1. Introduction

The study of oxide semiconductors intensified during the last years, due to their attractive physical properties. Thus, bismuth trioxide, Bi_2O_3 was found to be a semiconducting material which possesses beside a rather wide bandgap, high values of it's refractive index and dielectric permittivity, significant photoluminescence and UV photosensitivity [1]. It's potential applications are in the field of gas sensors, fuel cells, optical coatings or ceramic glass manufacturing. But care must be taken because Bi_2O_3 has five polymorphic forms, whose presence in a thin film strongly depends on the preparation conditions.

Another semiconductor oxide that captured the scientists' attention was antimony trioxide, Sb_2O_3. This oxide also has a wide bandgap and a very high electrical resistance, which recommend it for applications in the fields of: solar cells, light-emitting devices, flat panel displays, etc [2, 3].

Semiconducting materials with stratified crystalline heterostructures were studied in the last decade. Carefully controlled sandwich structures of two or more materials can give rise to novel properties not exhibited by the individual constituent layers. This opens the perspective of the use of the sandwich structures as thin films for coatings or for building-up parts of nanoelectronic devices.

More than one method was employed to prepare such overlapped structures [4-6]. Among these, vacuum thermal evaporation occupies an important place, because it can be easily controlled and it's rather inexpensive. The deposition conditions: nature and temperature of the substrate, pressure of and nature of the gas inside the deposition chamber, the deposition rate, etc can be varied in order to obtain thin films with more or less different characteristics.

After films preparation, it is essential to analyze them from different points of view, from which the structural and optical properties prove to be very important. The key is to find a correlation between the structural characteristics and/or structural changes of the prepared material, such as overlapped thin films heterostructures, due to changes in their deposition parameters with respect to their physico-chemical properties.

This article presents some of the results obtained for sandwich heterostructures between bismuth trioxide and antimony trioxide, prepared by classic thermal evaporation in vacuum. The study concerns the structure and the optical properties of the films. It was found out that both the temperature of the substrate and the order of deposition of the two employed oxides strongly influence the properties of the sandwich structures. Clear correlations between the structural characteristics extracted from the XRD patterns and the optical parameters inferred from the optical transmission spectra are pointed out.

2. Experimental

Individual bismuth trioxide and antimony trioxide thin films were prepared by vacuum thermal evaporation in a standard vacuum unit, at $8 \cdot 10^{-5}$ torr pressure. Thus, high purity (99,99%) bismuth trioxide and antimony trioxide from Sigma Aldrich were evaporated from a quartz ampoule surrounded by metallic wire, run by electric current. The substrates were high-quality cleaned glass slides.

Superimposed structures of the two different oxides were obtained by depositing a second oxide film by vacuum thermal evaporation on top of a first oxide film deposited on glass substrate.

The temperature of the glass substrates was monitored by a digital thermocouple. At each oxide deposition, the substrate temperature was kept at three different values, namely at 20^0C, 50^0C and 120^0C, respectively. Thus, the influence of the substrate temperature on the properties of the superimposed films was studied. Care was taken that the rest of the deposition parameters would remain the same for each deposition stage. Only the value of the electric current through the electric wire surrounding the evaporation ampoule was changes from 11 A for Bi_2O_3 deposition to 10.5 A for Sb_2O_3 deposition, due to the difference between the evaporation temperatures of the two oxides, *i. e.* 824^0 C for Bi_2O_3 and 656^0 C for Sb_2O_3, respectively.

Also, the deposition order of the two oxides was reversed, in order to find if there is any change in the properties of the entire two oxides structure.

The structure of the overlapped oxides was studied by means of X-ray Diffractometry. An XRD 6000 Shimadzu Diffractometer was used, which operates with a Cu target, at U=40 kV and I=30 mA, emitting the Cu-Kα line (λ=1.5418 Å). The scanning range was between 15 and 80 degrees, in order to capture XRD peaks from each deposited oxide. The scanning speed was of 2 degrees per minute and the 2 theta arrangement was employed. The XRD peaks were identified according to literature.

The highest peak of each XRD pattern was fitted very well by means of the Gauss function. The integral intensity and the integral width of that specific peak were deduced from the fittings. Then, the mean grain size was estimated according to Scherrer's formula:

$$D = \frac{0.94 \cdot \lambda}{\beta_{int} \cdot \cos\theta} \tag{1}$$

where λ is the wavelength of the X-rays used to obtain the XRD spectra, θ is the X-ray diffraction angle corresponding to the highest XRD peak, number 0.94 is used for spherically-assumed crystallites and β_{int} is the integral width of the XRD peak, *i. e.* the ratio between the integral intensity I_{int} of the XRD peak and the peak's height, I_M:

$$\beta_{int} = \frac{I_{int}}{I_M} \tag{2}$$

Optical transmission spectra for the obtained oxide films were acquired at room temperature with a Perkin Elmer Lambda 35 UV/VIS Spectrometer, at normal incidence, in the 190 nm – 1100 nm spectral range, with a 2 nm slit width.

Because the profile of the optical transmission spectra exhibited obvious maxima and minima, their analysis was done accordingly to the Swanepoel method [7-9]. Thus, the convolution curves (denoted by some as *envelopes*) of the interference maxima, T_M and minima, T_m were fitted as smooth, continuously rising curves. Then an interpolation at each 10 nm was performed and the values of the transmission maxima and minima were read from those convolution curves.

According to Swanepoel's method, the refractive index was computed from the following formula:

$$n = \left[N + \left(N^2 - s^2 \right)^{1/2} \right]^{1/2} \tag{3}$$

where s is the refractive index of the substrate, calculated from:

$$s = \frac{1}{T_s} + \left(\frac{1}{T_s^2} - 1 \right)^{1/2} \tag{4}$$

with T_s being the transmittance of the substrate alone. N in formula (3) is given by:

$$N = 2 \cdot s \cdot \frac{T_M - T_m}{T_M \cdot T_m} + \frac{s^2 + 1}{2} \tag{5}$$

All the graphs were plotted by means of the Microcal Origin program, which was also used to perform the fittings.

3. Results and discussion

The resulting overlapped XRD patterns for the sandwich structures made of Glass/Bi_2O_3/Sb_2O_3, denoted as: G_Bi_2O_3_Sb_2O_3, corresponding to three substrate temperatures are presented in Fig. 1.

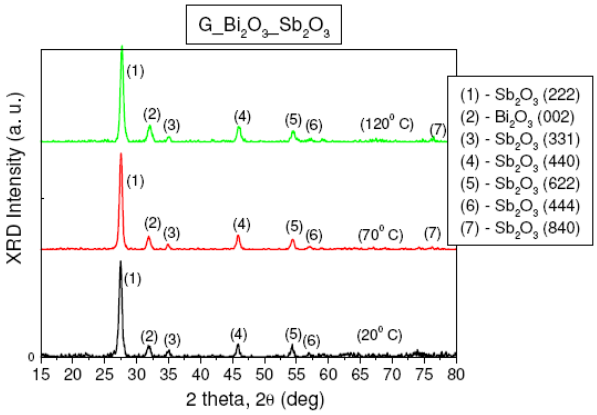

Fig. 1. X-ray diffraction patterns for G_Bi_2O_3_Sb_2O_3 sandwich structures at three substrate temperatures.

Table 1 reunites the parameters obtained from the fitting of the most prominent peak around $2\theta \approx 27.5$ deg. from Fig. 1 with a Gaussian function, as showed in Fig. 2, for each of the three chosen substrate temperatures. The magnitudes in table 1 represent: the position of the peak's maximum, $2\theta_M$, the integral intensity I_{int} of the peak, the height of the curve's peak, I_M at $2\theta_M$, the width of the peak

given by the fitting procedure, denoted as β_{fit}, expressed in degrees and the FWHM-full width half medium deduced from the Gaussian fitting as:

$$FWHM = 2 \cdot \sqrt{2 \cdot \ln 2} \cdot \beta_{fit} \quad (6)$$

Also, in table 1, β_{int} represents the integral width, computed both in degrees and in radians, according to formula (2) and <D> is the mean crystallite diameter, calculated according to Scherrer's formula (1) and expressed in nanometers.

The following inequalities can be inferred from Table 1:

$$2\theta_{M,20} < 2\theta_{M,70} < 2\theta_{M,120} \quad (7)$$

$$I_{int\,70} < I_{int\,20} < I_{int\,120} \quad (8)$$

$$I_{M,20} < I_{M,120} < I_{M,70} \quad (9)$$

$$\beta_{int,20} > \beta_{int,120} > \beta_{int,70} \quad (10)$$

$$\langle D \rangle_{20} < \langle D \rangle_{120} < \langle D \rangle_{70} \quad (11)$$

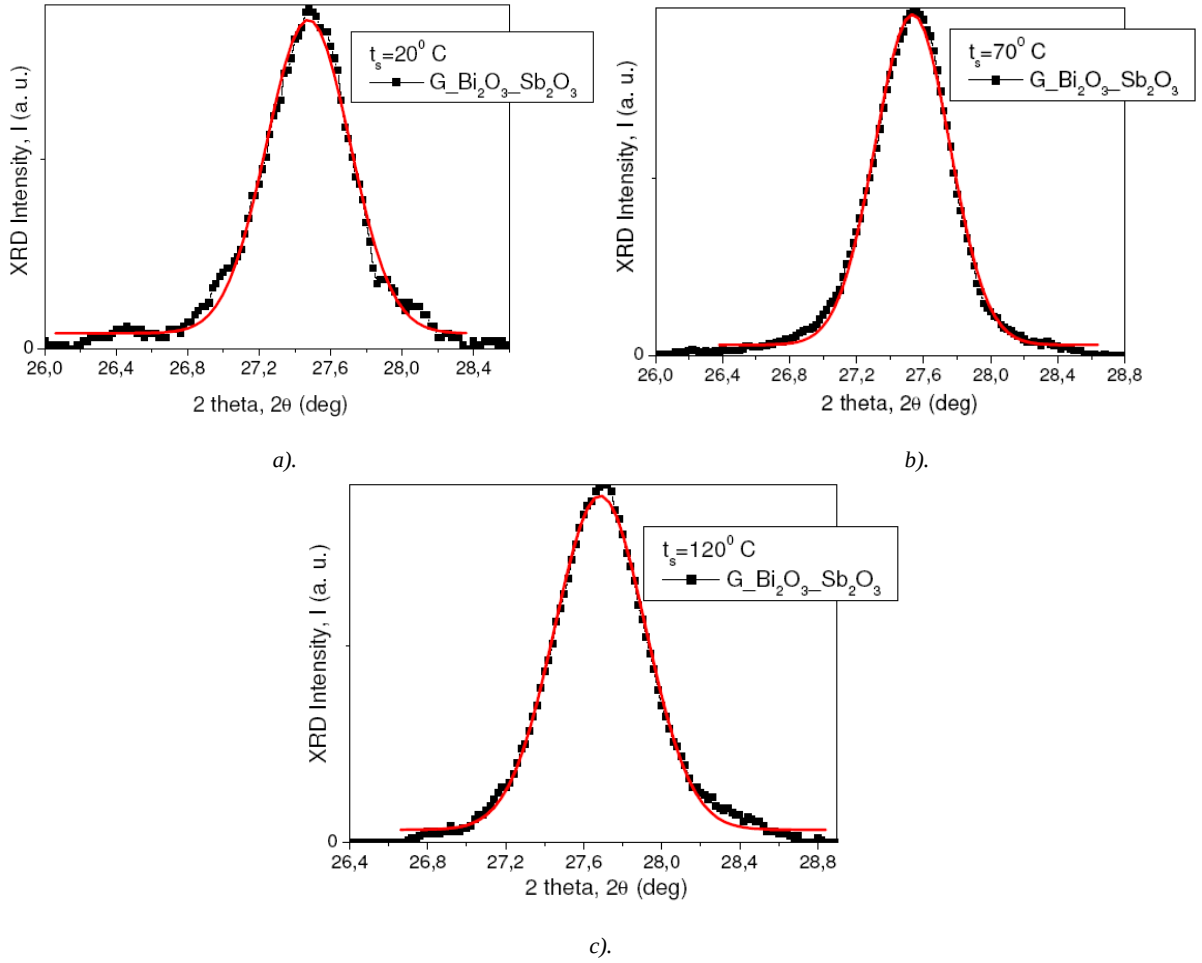

Fig. 2. Gaussian-function fitting of the most prominent peak in each of the three XRD patterns from Fig. 1.

Table 1. Parameters of the highest peak from the XRD patterns in Fig. 1 and mean grain diameter estimation

t_s (^{0} C)	$2\theta_M$ (deg.)	I_{int} (a. u.)	I_M (a. u.)	β_{fit} (deg.)	FWHM (deg.)	β_{int} (deg.)	β_{int} (rad.)	<D> (nm)
20	27.476	53.390	91.177	0.46721	1.1002	0.5856	0.0102	14.6272
70	27.533	53.085	95.195	0.44494	1.0478	0.5576	0.0097	15.3831
120	27.684	54.628	93.458	0.46638	1.0982	0.5845	0.0102	14.6337

The XRD pattern for the reversed-order overlapped bismuth and antimony trioxide, *i. e.* the sandwich structure made of Glass/Sb_2O_3/Bi_2O_3, denoted as: G_Bi_2O_3_Sb_2O_3 is presented in Fig. 3, at the same three substrate temperatures, specified in the insites of the figures. Correspondingly, the fitting of the highest peak in each XRD pattern from Fig. 3 with a Gauss curve is presented in Fig. 4. This peak, found at around $2\theta \approx 27.7$ deg. belongs, as to be expected, to Bi_2O_3, which is on top of the overlapped structure. Table 2 reunites the parameters resulting from the fittings in Fig. 4. The magnitudes in table 2 are similar to those in table 1.

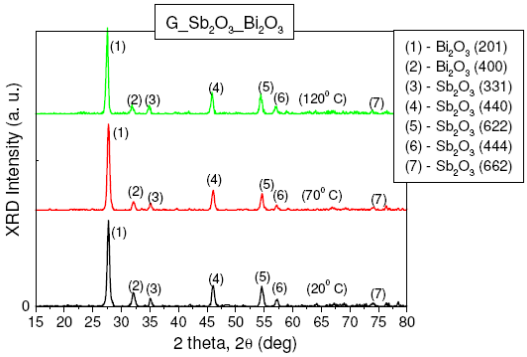

Fig. 3. X-ray diffraction patterns for G_Sb_2O_3_Bi_2O_3 sandwich structures at three substrate temperatures.

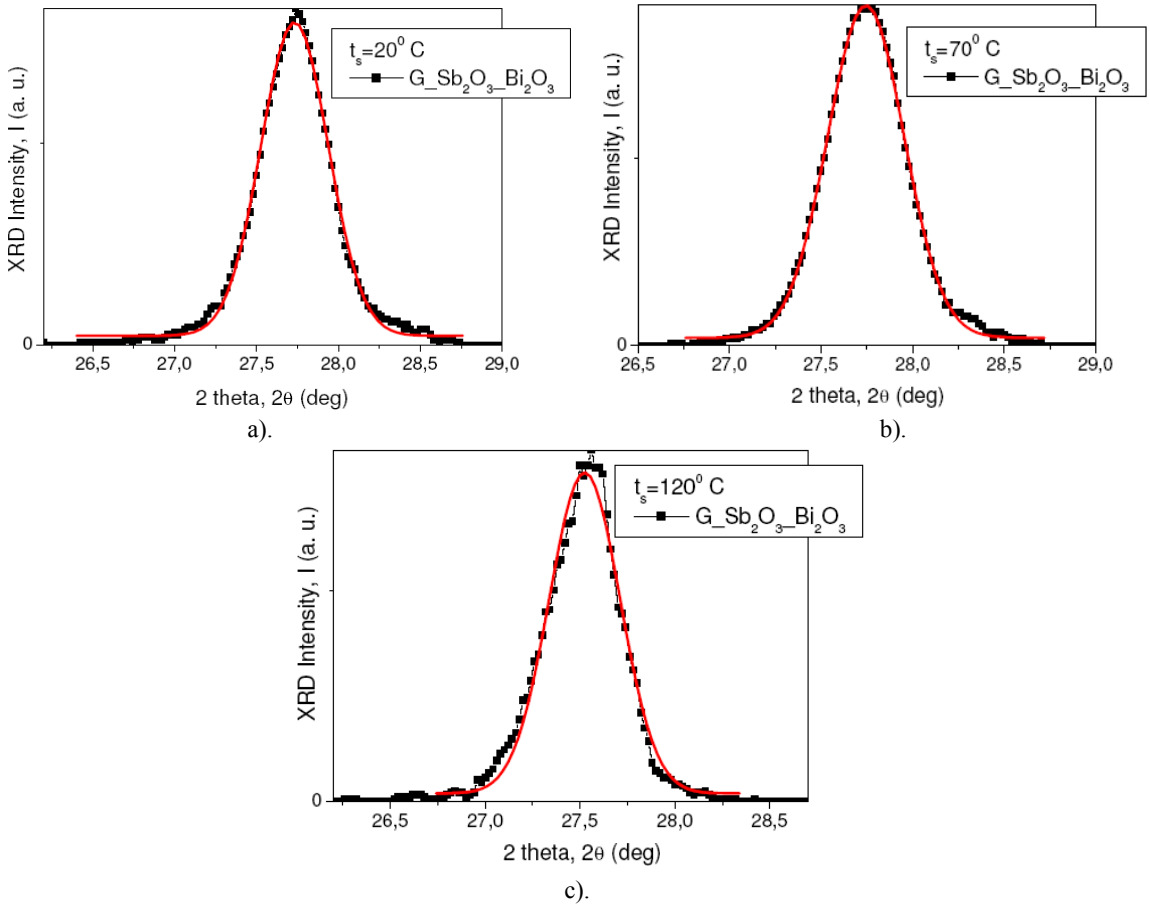

Fig. 4. Gaussian-function fitting of the most prominent peak in each of the three XRD patterns from Fig. 3.

Table 2 Parameters of the highest peak from the XRD patterns in Fig. 2 and mean grain diameter estimation

t_s (^{0} C)	$2\theta_M$ (deg.)	I_{int} (a. u.)	I_M (a. u.)	β_{fit}	FWHM (deg.)	β_{int} (deg.)	β_{int} (rad.)	<D> (nm)
20	27.732	48,173	93.189	0.41246	0.9713	0.5169	0.0090	16.5866
70	27.745	51.097	97.377	0.41868	0.9859	0.5247	0.0091	16.4049
120	27.524	42.792	91.372	0.37367	0.8799	0.4683	0.0082	18.1967

The following inequalities can be inferred from table 2:

$$2\theta_{M,120} < 2\theta_{M,20} < 2\theta_{M,70} \quad (12)$$

$$I_{int,120} < I_{int,20} < I_{int,70} \quad (13)$$

$$I_{M,120} < I_{M,20} < I_{M,70} \quad (14)$$

$$\beta_{int,70} > \beta_{int,20} > \beta_{int,120} \quad (15)$$

$$\langle D \rangle_{70} < \langle D \rangle_{20} < \langle D \rangle_{120} \quad (16)$$

The investigation of the crystalline structure of the overlapped films, done by XRD proves that the deposited oxide thin films are multi-phase and polycrystalline.

Also, not only peaks from the top oxide are present in the XRD pattern, but also peaks from the bottom oxide are obtained, even though their intensity is much diminished due to the long path of the X-rays till the oxide film from the bottom of the heterostructures.

Moreover, a clear tendency of texturising, *i. e.* a specific preferential orientation of the crystallites of each top oxide layer was noticed, since there is a more prominent XRD peak than the others in each XRD pattern.

The average size of the crystalline grains obtained from the fitting of the highest XRD peak is between 14.6 and 18.2 nm. The G_Bi_2O_3_Sb_2O_3 heterostructures exhibit the biggest nanocrystallites at $t_s = 70^0$ C substrate temperature, while, the G_Sb_2O_3_Bi_2O_3 have, at the same t_s, the smallest nanocrystallites.

In any order of oxide deposition, the heterostructures show a kind of reversibility from the point of view of I_{int}, I_M and $\langle D \rangle$,when passing from 20^0 C, to 70^0 C and 120^0 C substrate temperature.

Passing to the spectral analysis, Fig. 5 exhibits the spectra of the transmittance of the optical radiation through the G_Bi_2O_3_Sb_2O_3 sandwich structures at the same three substrate temperatures, along with the convoluting curves for the interference maxima and minima, respectively, according to Swanepoel's method, from where the refractive index of each heterostructure was computed.

The values of the transmittance, T of the G_Bi_2O_3_Sb_2O_3 heterostructures increase when passing from 20^0 C, to 70^0 C substrate temperature, then it diminishes at 120^0 C substrate temperature. This is the same kind of reversible behavior as noticed for the average nanocrystallites size, $\langle D \rangle$. This could be explained by the fact that, at 70^0 C substrate temperature, because the grains are bigger, the diffusion of light at grain limits is reduced and this way, a bigger part of the incident optical radiation is transmitted through the heterostructures. Also, one can suppose that there's maybe an interchange between the crystalline phases of the bottom layer of bismuth trioxide when the substrate temperature changes. This aspect will be further studied and verified.

After computing the refractive index of the superimposed oxides, the Wemple-DiDomenico method for the dispersion of the refractive index was applied. Thus, the $\frac{1}{n^2-1} = f\left[(h\cdot\nu)^2\right]$ dependence was calculated and plotted in Microcal Origin, being expected to give a linear shape, with negative slope, according to the Wemple-DiDomenico relation:

$$n^2(\nu) = 1 + \frac{E_d \cdot E_0}{E_0^2 - (h\cdot\nu)^2} \quad (17)$$

where E_d and E_0 are the oscillator energy and strength, respectively for the single-oscillator model [8].
If the equation of the linear fitting of

$$\frac{1}{n^2-1} = f\left[(h\cdot\nu)^2\right] \text{ is: } y = A + B\cdot x \quad (18),$$

where:

$$x = (h\cdot\nu)^2 \text{ and } y = \frac{1}{n^2-1} \quad (19),$$

then, by inferring from formula (17), E_d and E_0 can be calculated as:

$$E_d = \frac{1}{\sqrt{(-A\cdot B)}} \text{ and } E_0 = E_d \cdot A \quad (20)$$

From here, the estimation of the bandgap energy E_g can be done according to:

$$E_g = \frac{E_0}{2} \quad (21).$$

Fig. 6 presents the superimposed dispersion curves type $\frac{1}{n^2-1} = f\left[(h\cdot\nu)^2\right]$, proposed by Wemple-DiDomenico, for the three heterostructures of G_Bi_2O_3_Sb_2O_3.

Table 3 presents the fitting parameters and corresponding absolute error for the graphs in Fig. 6, *i. e.* the ordinate at the outset, A and the slope, B of the linear fittings of the almost linear parts of the graphs in Fig. 6.

Then, table 4 presents the values of the oscillator energy, E_d and oscillator strength, E_0 deduced from formulas (20). Also, the estimation of the energy bandgap, E_g of the heterostructures are given in table 4, according to (21).

The same kind of reversibility of the energy bandgap, E_g of the G_Bi_2O_3_Sb_2O_3 heterostructures is noticed when passing from 20^0 C, to 70^0 C and 120^0 C substrate temperature as noticed for the average grain size $\langle D \rangle$. Thus, at $t_s = 70^0$ C, E_g is the biggest, being estimated of 2.98 eV (see table 4).

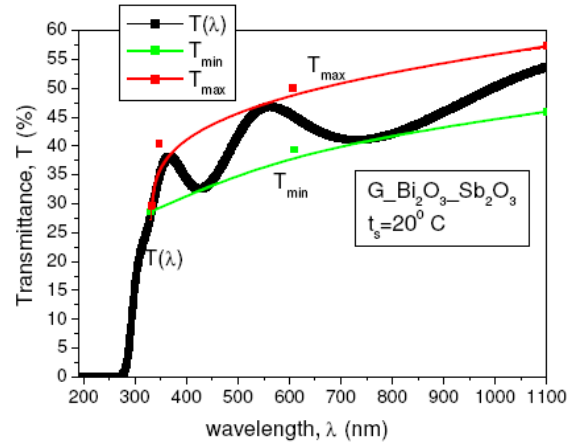

a

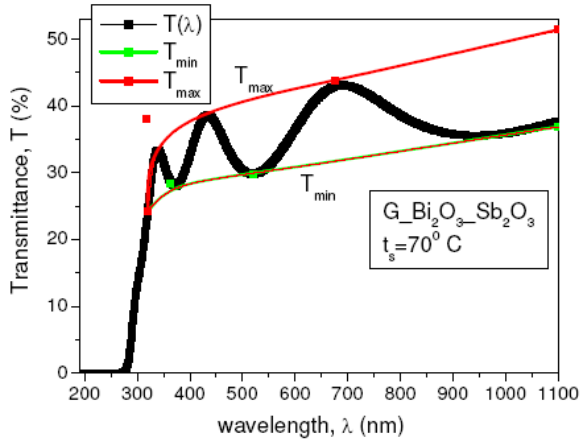

b

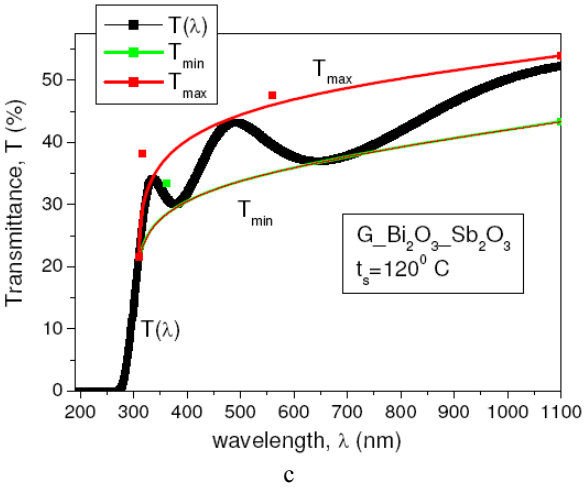

c

Fig. 5. Optical transmission spectra for G_Bi_2O_3_Sb_2O_3 sandwich structures at three substrate temperatures: a).20^0 C; b). 70^0 C; c). 120^0 C.

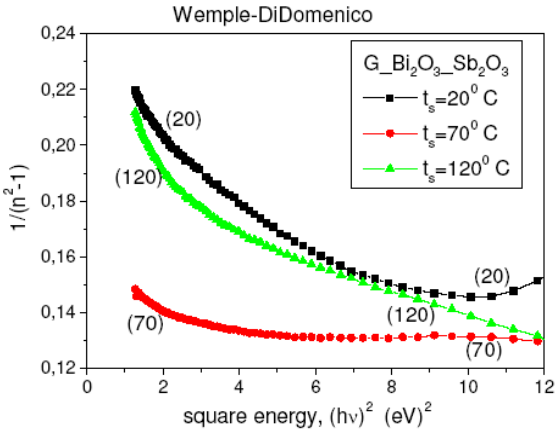

Fig. 6. Dispersion curves according to Wemple-DiDomenico method for G_Bi_2O_3_Sb_2O_3 sandwich structures at three substrate temperatures.

Table 3 Fitting parameters and corresponding absolute error for the graphs in Fig. 6

t_s (^{0} C)	A	Error on A ($\cdot 10^4$)	B	Error on B ($\cdot 10^4$)
20	0.21935	6.76131	-0.00967	1.5847
70	0.14369	3.34448	-0.00245	0.904815
120	0.18916	5.76543	-0.00531	0.989004

Table 4 Parameters deduced according to Wemple-DiDomenico method for G_Bi_2O_3_Sb_2O_3 sandwich structures at three substrate temperatures

t_s (^{0} C)	E_d (eV)	E_0 (eV)	E_g (eV)
20	21.7129	4.7627	2.3814
70	53.2971	7.6583	3.8291
120	31.5528	5.9685	2.9843

The same kinds of optical analysis are done for the G_Sb_2O_3_Bi_2O_3 heterostructures. Thus, figs. 7 present the optical transmission spectra with the convoluting curves of the interference maxima and minima, respectively. Swanepoel's method was also employed for refractive index calculations.

This time, the interference patterns are much diminished than in the case of G_Bi_2O_3_Sb_2O_3 sandwich structures, but the over all values of the transmission factor are bigger when Bi_2O_3 is on top of the heterostructures.

There is also here a small decrease of the over all optical transmittance at $t_s = 70^0$ C as compared to the transmission spectra for the heterostructures with $t_s = 20^0$ C and $t_s = 120^0$ C, respectively, as also noticed for the G_BiO_3_Sb_2O_3 samples.

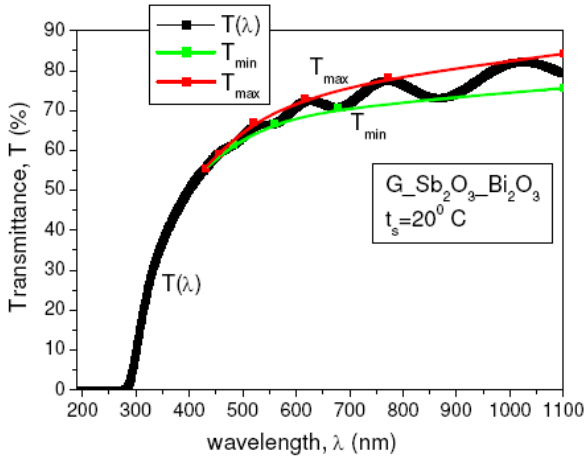

a

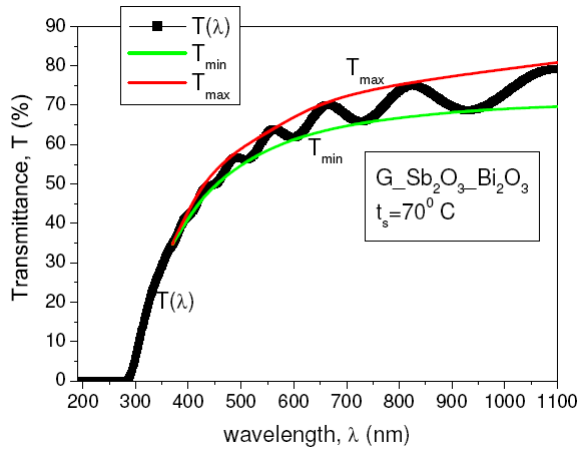

b

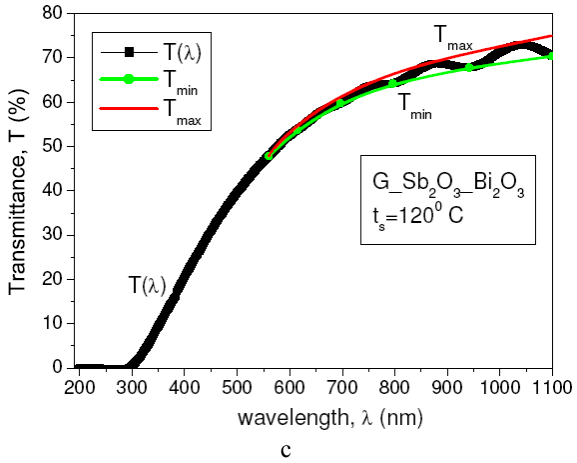

c

Fig. 7. Optical transmission spectra for $G\_Sb_2O_3\_Bi_2O_3$ sandwich structures at three substrate temperatures: a). 20^0 C; b). 70^0 C; c). 120^0 C.

Correspondingly, Fig. 8 exhibits the dispersion curves type $\frac{1}{n^2-1} = f\left[(h\cdot\nu)^2\right]$, proposed by Wemple-DiDomenico, for the three heterostructures of $G\_Sb_2O_3\_Bi_2O_3$. As it can be noticed, in the case of $G\_Sb_2O_3\_Bi_2O_3$ heterostructures, there are serious deviations from the aspect of negative slope linear parts of the plots proposed by Wemple-DiDomenico.

Table 5 presents the fitting parameters and corresponding absolute error for the graphs in Fig. 8, *i. e.* the ordinate at the outset, A and the slope, B of the linear fittings of the almost linear parts of the graphs in Fig. 8, there where small negative slope linear parts of the plots were found. At $t_s = 120^0$ C there is no error for A and B because the linear fitting was done exactly for the two points from the plot which exhibit a negative slope.

Table 6 presents the estimations of E_d, E_0 and energy bandgap, E_g for the $G\_Sb_2O_3\_Bi_2O_3$ samples, calculated from (20) and (21), respectively.

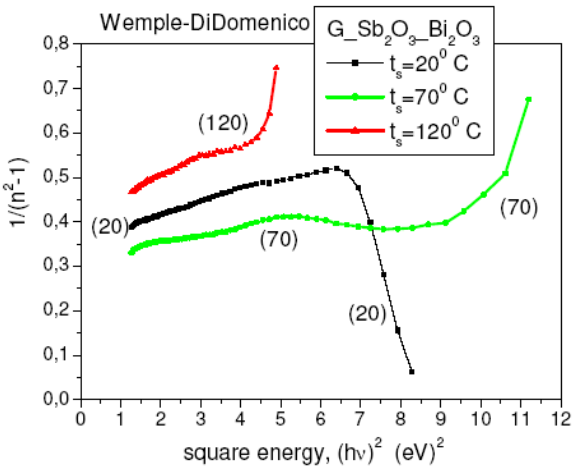

Fig. 8. Dispersion curves according to Wemple-DiDomenico method for $G\_Sb_2O_3\_Bi_2O_3$ sandwich structures at three substrate temperatures.

The energy bandgap shows even in the case of $G\_Sb_2O_3\_Bi_2O_3$ heterostructures the reversible behavior with respect to the change of substrate temperature. At $t_s = 70^0$ C the energy bandgap is the highest, being estimated at 2.93 eV. It can be also supposed that there is a link between the variation of the energy bandgap and the mean grain size, $\langle D \rangle$. But, in the case of $G\_Sb_2O_3\_Bi_2O_3$, at $t_s = 70^0$ C, $\langle D \rangle$ is the smallest, so the explanation with intergrain diffusion of light doesn't stand. Another explanation is yet to be found.

Table 5 Fitting parameters and corresponding absolute error for the graphs in Fig. 8

t_s (^{0} C)	A	Error on A	B	Error on B
20	2.68925	0.09231	-0.31809	0.01214
70	0.48947	0.00828	-0.01425	0.00123
120	0.65475	-	-0.02248	-

Table 6. Parameters deduced according to Wemple-DiDomenico method for G_Sb_2O_3_Bi_2O_3 sandwich structures at three substrate temperatures

t_s (^{0} C)	E_d (eV)	E_0 (eV)	E_g (eV)
20	1.0812	2.9076	1.4538
70	11.9737	5.8608	2.9304
120	8.2426	5.3968	2.6984

4. Conclusions

Sandwich heterostructures of Bi_2O_3 and Sb_2O_3 were prepared by vacuum thermal evaporation on glass slides in both orders. Their structure proved to be polycrystalline from the analysis of the XRD patterns. The estimation of the crystallites size was done. The optical transmission properties were also studied, by using the Swanepoel and the Wemple-DiDomenico methods. The substrate temperature and the order of deposition of the two different oxides proved to strongly influence the properties of the resulting sandwich heterostructures. Connections between the reversible behaviors of the values for the energy bandgap and of the mean crystallites size with respect to the change in substrate temperature were found.

References

[1] L. Leontie, J. Optoelectron. Adv. Mater. **8**(3), 1221 (2006).
[2] N. Tigau, V. Ciupina, G. Prodan, G. I. Rusu, C. Gheorghies, E. Vasile, J. Optoelectron. Adv. Mater. **15 (4),** 907 (2003).
[3] N. Tigau, Rom. Journ. Phys. **53**(1-2), 203 (2008).
[4] Z. D. Kovalyuk, V. M. Katerynchuk, O. M. Sydor, J. Optoelectron. Adv. M. **7**(2), 903 (2005).
[5] N. Tigau, V. Ciupina, G. Prodan, G. I. Rusu, C. Gheorghies, E. Vasile, J. Optoelectron. Adv. Mater. **15**(4), 907 (2003).
[6] M. H. Islam, C. A. Hogarth, Phys. Stat. Sol. **99**, 503 (1986).
[7] R. Swanepoel, J. Phys. I: Sci. Instrum. **16**, 1214 (1983).
[8] E. Marquez, J. B. Ramirez-Malo, P. Villares, R. Jimenez-Garay, R. Swanepoel, Thin Solid Films **254**, 83 (1995).
[9] D. Sharma, P. Sharma, N. Thakur, J. Optoelectron. Adv. Mater. – Rapid. Comm. **3**(2), 145 (2009).
[10] L. Meng, M. Andritschky, M. P. dos Santos, Thin Solid Films **223**, 242 (1993).

*Corresponding author: sbotacond@yahoo.com